

# Probe R-parity violating stop resonance at the LHeC

---

**Wei Hong-Tang, Zhang Ren-You, Guo Lei, Han Liang, Ma Wen-Gan, Li Xiao-Peng  
and Wang Ting-Ting**

*Department of Modern Physics, University of Science and Technology of China, Hefei,  
Anhui 230026, P.R.China*

*E-mail: weiht@mail.ustc.edu.cn, zhangry@ustc.edu.cn,  
guolei@mail.ustc.edu.cn, hanl@ustc.edu.cn, mawg@ustc.edu.cn,  
qqpengal@mail.ustc.edu.cn, tingting@mail.ustc.edu.cn*

**ABSTRACT:** We investigate the possibility of detecting single squark production at the proposed LHeC collider, in the framework of R-parity violating supersymmetry. Taking advantage of the enhancement of the direct resonance production of squark and the distinctive kinematics distributions of  $\tilde{q} \rightarrow lq$  two body decay final states, the LHeC provides excellent opportunities of probing R-violating  $\hat{L}\hat{Q}\hat{D}$  interactions at unprecedented level compared to all the knowledge derived from indirect low energy nucleon measurements. If no apparent deviation from SM predictions on high invariant mass of muon and b-quark final states at the LHeC with  $1fb^{-1}$  data, the sensitivities on  $\hat{L}\hat{Q}\hat{D}$  coupling constant  $\lambda'_{131} \times \lambda'_{233}$  can be improved by nearly four orders, at energy scale about 100 GeV.

**KEYWORDS:** LHeC, R-parity violating (RPV) interactions, Stop

**PACS:** 12.60.Jv, 11.30.Fs, 13.85.Fb, 13.85.Rm.

---

## Contents

1. Introduction	1
2. Signal and Background at the <i>LHeC</i>	2
3. Event Selection and Discussion	5
4. Summary	7

---

## 1. Introduction

In the current structure of the Standard Model (SM), the conservations of baryon number  $B$  and lepton number  $L$  are automatic consequence of the gauge invariance and renormalizability. On the other hand, neutrino oscillation observations [1–3] manifest strong lepton flavor violation, and imply that the SM is not a fundamental particle theory and should be extended. In minimal supersymmetric (SUSY) extensions of the SM, a new multiplicative quantum number,  $R = (-1)^{2S+L+3B}$ , is introduced in terms of  $B$ ,  $L$  and the spin quantum number  $S$ , to distinguish the SM particles ( $R = +1$ ) from their SUSY partners ( $R = -1$ ). In the most general supersymmetric potential,  $R$ -parity violating (RPV) interactions can be included as

$$\mathcal{W}_{\cancel{R}_p} = \frac{1}{2}\epsilon_{ab}\lambda_{ijk}\hat{L}_i^a\hat{L}_j^b\hat{E}_k + \epsilon_{ab}\lambda'_{ijk}\hat{L}_i^a\hat{Q}_j^b\hat{D}_k + \frac{1}{2}\epsilon_{\alpha\beta\gamma}\lambda''_{ijk}\hat{U}_i^\alpha\hat{D}_j^\beta\hat{D}_k^\gamma + \epsilon_{ab}\delta_{i\mu_i}\hat{L}_i^a\hat{H}_2^b \quad (1.1)$$

where  $i,j,k=(1,2,3)$  are generation indices,  $a,b=(1,2)$  are  $SU(2)$  isospin indices, and  $\alpha,\beta,\gamma$  are  $SU(3)$  color indices.  $\hat{L}$  and  $\hat{Q}$  are the lepton and quark  $SU(2)$  doublet superfields,  $\hat{E}$ ,  $\hat{U}$  and  $\hat{D}$  denote the singlets, and  $\hat{H}$  is the Higgs doublet. The bilinear terms  $\hat{L}\hat{H}$  mix the lepton and Higgs superfield with the Higgsino mass parameter  $\mu$ , and consequently generate masses of neutrinos. All the trilinear terms,  $\hat{L}\hat{L}\hat{E}$ ,  $\hat{L}\hat{Q}\hat{D}$  and  $\hat{U}\hat{D}\hat{D}$  with dimensionless  $R$ -violating Yukawa couplings  $\lambda$ ,  $\lambda'$  and  $\lambda''$  respectively, only violate either  $L$ - or  $B$ -symmetry alone. Constraints on RPV couplings obtained so far are well summarized in Ref. [4].

Along with introducing compatible description of neutrino oscillation in a natural way, the most attracting phenomena of RPV is to allow single production of SUSY particles. Contrary to the pair productions of SUSY particles in the  $R$ -conserved frame, the RPV resonance production at colliders would dramatically reduce the threshold of probing new physics. There were studies of sneutrino resonance production and decay at next generation  $e^+e^-$  linear colliders [5] and at hadron colliders by both theoretical discussion [6–8] and experimental measurements at the Tevatron [9, 10], via lepton flavor violating  $\hat{L}\hat{L}\hat{E}$  and  $\hat{L}\hat{Q}\hat{D}$  interactions. For single squark production, stringently constrained by indirect

low energy nucleon experiments, the baryon number violating  $\hat{U}\hat{D}\hat{D}$  couplings are negligibly small, for example  $\lambda''_{11k}$  are less than  $10^{-7}$  given by nucleon-antinucleon oscillation measurements, and thus mechanics of RPV squark resonance production at TeV hadron colliders are highly suppressed. On the other hand, at the proposed Large Hadron electron Collider (LHeC) [11], which provides complement to the LHC by using the existing 7 TeV proton beam, single squark can be produced and detected via  $\hat{L}\hat{Q}\hat{D}$  couplings in the next generation of electron-proton  $e^-p$  collision experiments. In this paper we investigate the potential of searching stop quark via  $e^- + p \rightarrow \tilde{t}_1^* \rightarrow \mu^- + \bar{b}$  resonance process, which provides a new prospect to probe the RPV lepton flavor violating interactions.

## 2. Signal and Background at the LHeC

Under the single dominance hypothesis [4] that  $\tilde{t}_1$ , the lighter mass eigenstate of the two stop quarks, is simply governed by  $\hat{L}\hat{Q}\hat{D}$  couplings  $\lambda'_{131}$  and  $\lambda'_{233}$ , the parton-level signal process can be denoted as  $e^-(p_1) + \bar{d}(p_2) \rightarrow \tilde{t}_1^* \rightarrow \mu^-(p_3) + \bar{b}(p_4)$ , depicted by the Feynman diagram in FIG. 1.

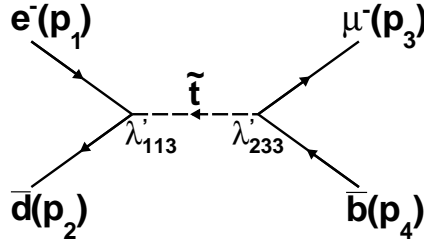


**Figure 1:** The parton-level Feynman diagram of RPV signal  $e^- \bar{d} \rightarrow \mu^- \bar{b}$ .

The amplitude of the signal process at parton-level can be written as

$$\mathcal{M} = \bar{v}(p_2) \left[ \lambda'_{131} \frac{1 - \gamma^5}{2} \right] u(p_1) \cdot \frac{-i}{\hat{s} - M^2 + iM\Gamma} \cdot \bar{u}(p_3) \left[ \lambda'_{233} \frac{1 - \gamma^5}{2} \right] v(p_4) \quad (2.1)$$

where  $\sqrt{\hat{s}} = M_{\mu b}$  is the center-of-mass energy of the hard scattering and equivalent to the final state invariant mass. The parameter  $M$  and  $\Gamma$  denote the mass and total width of the lighter stop quark  $\tilde{t}_1$  respectively, while the lighter stop is assumed only decaying through  $ed$  and  $\mu b$  modes.

$$\Gamma = \frac{\lambda'_{233}{}^2}{16\pi} \cdot \frac{(M^2 - m_b^2)^2}{M(M^2 + m_b^2)} + \frac{\lambda'_{131}{}^2}{16\pi} \cdot M \quad (2.2)$$

The parton-level differential cross section for signal in the rest frame of final muon and b-quark states can be written as

$$\frac{d\hat{\sigma}}{d\Omega} = \frac{(\lambda'_{131}\lambda'_{233})^2}{(16\pi)^2\hat{s}} \frac{(\hat{s} - m_b^2)^2}{(\hat{s} - M^2)^2 + (\Gamma M)^2} \quad (2.3)$$

For the particle level signal process  $e^- + p \rightarrow \tilde{t}_1^* \rightarrow \mu^- + \bar{b}$  at the LHeC, the cross section and kinematic distributions can be obtained by convoluting the parton-level subprocess with the parton distribution function (PDF) of the proton.

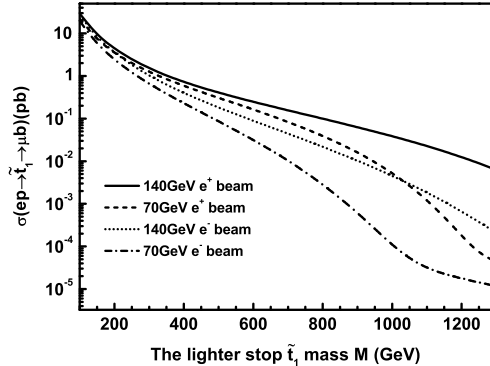


**Figure 2:** The cross sections for stop resonance production  $\sigma(ep \rightarrow \tilde{t}_1 \rightarrow \mu b)$  at the LHeC as functions of stop mass.

The indirect two standard deviation bounds on the coupling constants and the mass of stop are given as [4]

$$\lambda'_{131} \leq 0.03, \quad \lambda'_{233} \leq 0.45, \quad M \geq 100 \text{ GeV} \quad (2.4)$$

This set of parameter limitations will be used as default for demonstration purpose unless explicitly stated otherwise.

There exist options of lepton beam configuration, namely electron or positron beam with 70 or 140 GeV energy. Positron beam configurations are taken into account as comparisons with their charge-conjugated electron beams. The signal cross sections evaluated under different beams as a function of stop quark mass are depicted in FIG. 2. The positron beam options raise larger cross sections for the signal  $e^+ + d \rightarrow \tilde{t}_1 \rightarrow \mu^+ + b$  than those for its charged-conjugated process in most mass region, simply because of large density of high energy valance d-quark in proton PDF. To have our discussion conservative, we take 70 GeV electron beam as default except stating explicitly otherwise.

To simulate the kinematics of the RPV signal and SM predictions, the COMPHEP [12] event generator and CTEQ6L1 [13, 13] PDF are used. The reducible SM background in electron beam configuration comes from  $e^- + p \rightarrow e^- + b/\bar{b} \rightarrow \nu_e + b/\bar{b} + W^-$ , where the on-shell W boson decays leptonically via  $\mu^- \bar{\nu}_\mu$  channel. Since from experimental point of view, it is difficult to determine the original charge of quarks in reconstructed jets, both  $b$  and  $\bar{b}$ -quark initial state contributions at parton-level should be taken into account as background to the muon and b-jet associated signal. However, a real (virtual) top-quark could be produced via  $e^- + \bar{b} \rightarrow \nu_e + \bar{t}^{(*)}$ , and enhance the cross section greatly in the  $\bar{b}$ -quark channel against  $b$ -quark contribution, i.e.  $\hat{\sigma}(e^- + \bar{b} \rightarrow \nu_e + W^- + \bar{b})$  is about two order greater in magnitude than  $\hat{\sigma}(e^- + b \rightarrow \nu_e + W^- + b)$  in most kinematic region. Therefore, we only choose  $e^- + p \rightarrow \nu_e + W^- + \bar{b}$  in electron beam and its charge conjugation  $e^+ + p \rightarrow \bar{\nu}_e + W^+ + b$  in positron beam configuration as dominant SM background to  $e^\pm + p \rightarrow \mu^\pm + b/\bar{b}$  signal. In the numerical calculation we take  $m_e = 0.511 \text{ MeV}$ ,  $m_\mu = 105.658 \text{ MeV}$ ,  $m_W = 80.365 \text{ GeV}$ ,  $m_t = 173.5 \text{ GeV}$ ,  $m_b = 4.65 \text{ GeV}$ ,  $\Gamma_{total}^t = 2.0 \text{ GeV}$ ,

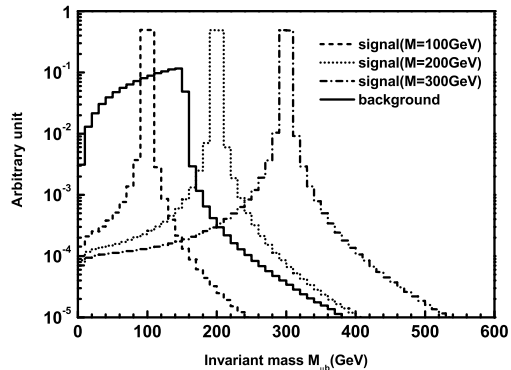


**Figure 3:** The invariant mass  $M_{\mu b}$  distributions of background and signals with 70GeV electron beam at the LHeC.

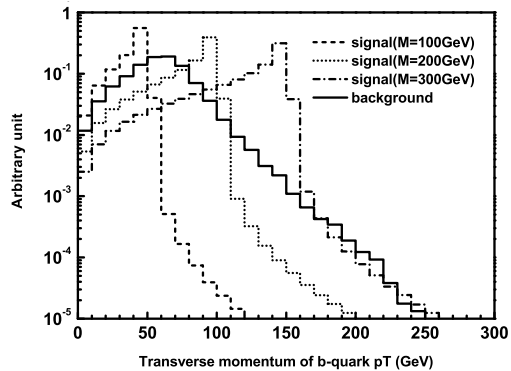


**Figure 4:** The b-quark transverse momentum distributions of background and signals with 70GeV electron beam at the LHeC.

$\alpha_{ew}^{-1} = 137.036$ , and set the factorization scales for signal and background processes as  $\mu_f = M$  and  $\mu_f = m_t$ , respectively.

In SM background, the two neutrinos  $\nu_e$  and  $\nu_\mu$  will escape detection, and result in significant missing transverse energy  $\cancel{E}_T$ . The remaining muon and b-quark are relatively soft, and would mimic the  $\mu + b$  signal. On the other hand, governed by RPV Yukawa couplings, the outgoing muon and b-quark in signal are isotropic in the rest frame of stop quark, and therefore the transverse momentum  $p_T$  of the two final state particles are inclined to be as hard as taking half of the stop mass. Accordingly, the signal is characterized by isolated and high  $p_T$  outgoing muon and b-jet, back-to-back in the transverse  $r - \phi$  plane, without sensible missing transverse energy. In experimental point of view, these features will help to distinguish signal from background. The comparisons of kinematic distributions of background and signals at the LHeC are given in FIG. 3 and FIG. 4. The distributions of the non-zero  $\cancel{E}_T$  and azimuthal separation of final muon and b-quark of background are shown in FIG. 5.

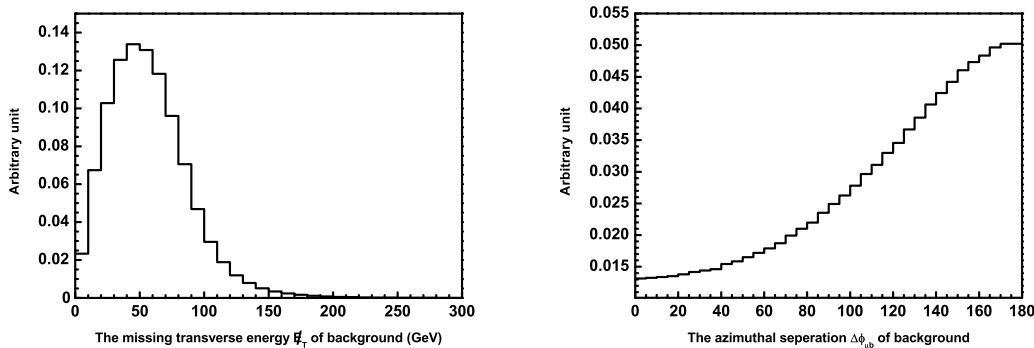


**Figure 5:** The distributions of  $\cancel{E}_T$  and the azimuthal separation  $\Delta\phi_{\mu b}$  of background with 70GeV electron beam at the LHeC.

### 3. Event Selection and Discussion

Taking advantage of distinction between the RPV SUSY and SM predictions on  $\mu + b + X$  final states, a strategy of event selection can be developed as

- Kinematics cuts: for muon,  $p_T^\mu > 25\text{GeV}$ ,  $|\eta_\mu| < 2.5$ ; for b-jet,  $p_T^b > 25\text{GeV}$ ,  $|\eta_b| < 3.5$ .
- The open angle in transverse plane  $\Delta\phi_{\mu b} > 2.94$ , in which the deviation from exact back-to-back of the muon and b-jet leaves room for the effect of initial state radiation and resummation in signal.
- The missing transverse energy veto as  $\cancel{E}_T < 25\text{ GeV}$ , taking possible energy resolution into account.
- The invariant mass  $M_{\mu b} > 85\text{ GeV}$ . This loose mass cut is to have the most efficiency of 100GeV stop, assuming  $3\sigma$  b-quark jet energy resolution below the resonance mass pole, and the cut will not be shifted for other signal mass point to derive most conservative estimation.
- A 60% b-tagging efficiency is assumed for b-jet identification in experiments.

If we assume the b-tagging efficiency is 100%, these criteria could suppress the SM background efficiently. Only about 5.85%  $\nu_e b W(\mu\nu_\mu)$  events will survive after taking above selection rules, which corresponds to a cross section of 9.65 fb. On the other hand, 86% signal events survive the above selections at stop mass  $M = 100\text{ GeV}$ , and the efficiency of signal would rise with the increment of stop mass from 100 GeV to 300 GeV. Assuming there is no apparent deviation from SM prediction of  $\mu + b$  final states, the  $2\sigma$  exclusion limits on signal can be derived, by simply using significance method  $\frac{S}{\sqrt{S+B}} \leq 2.0$ . TABLE 1 gives the cross sections of signal after event selection, and the minimum luminosity needed to draw  $2\sigma$  exclusion at RPV couplings given by Eq.(2.4), with  $e^\pm p$  collider options respectively.

The luminosities required to exclude stop  $\mu + b$  signal at a 70 GeV electron- or positron-proton LHeC collider are also depicted in FIG. 6. The obvious better sensitivity of positron

$M$ ( $GeV$ )	$\sigma(e^+p)$ ( $pb$ )	exclusion $\mathcal{L}(e^+p)$ ( $pb^{-1}$ )	$\sigma(e^-p)$ ( $pb$ )	exclusion $\mathcal{L}(e^-p)$ ( $pb^{-1}$ )
100	19.15	0.348	16.80	0.40
200	3.45	1.94	2.37	2.81
300	1.21	5.54	0.63	10.69
400	0.56	12.19	0.22	32.31
500	0.28	24.64	$7.82 \times 10^{-2}$	95.79
600	0.14	50.03	$2.73 \times 10^{-2}$	330.43
700	$6.94 \times 10^{-2}$	109.36	$8.52 \times 10^{-3}$	$1.69 \times 10^3$
800	$3.10 \times 10^{-2}$	282.27	$2.22 \times 10^{-3}$	$1.61 \times 10^4$

**Table 1:** The cross sections and the minimal luminosities of  $2\sigma$  exclusion at the LHeC with 70  $GeV$   $e^\pm$  beam.

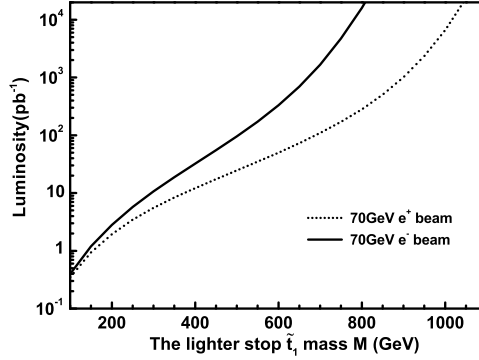


**Figure 6:** The expected luminosity for  $2\sigma$  exclusion of RPV signals at the LHeC.

beam in probing high mass RPV signal than that of electron beam, is simple raised by the larger parton density of valance  $d$ -quark than that of sea  $\bar{d}$ -quark in proton. One can see that with  $1fb^{-1}$  at 70  $GeV$   $e^-p$  collider, the RPV  $\mu + b$  resonance of stop quark can be excluded up to about  $M \leq 700 GeV$  with default RPV couplings.

New direct  $2\sigma$  upper bounds on  $\lambda'_{233}$  at given  $\lambda'_{131}$  can be calculated as a function of stop mass, and are depicted at 70 $GeV$  electron beam case in FIG.7. More stringent constraints on RPV couplings could be given at LHeC. For example, at energy scale about 100  $GeV$ , constraints as  $\lambda'_{131} = 0.005$ ,  $\lambda'_{233} \lesssim 0.85 \times 10^{-3}$  can be derived from exclusive  $\mu + b$  resonance search, which improve the associated sensitivity on  $\lambda'_{131} \times \lambda'_{233}$  by nearly 4 orders compared to those given in Eq.(2.4) from low energy processes. Moreover, in high mass region up to 500 $GeV$ , it is likely that either the stop RPV  $\mu + b$  resonance could be directly detected, or  $\hat{L}\hat{Q}\hat{D}$  couplings would be constrained much more stringently at the LHeC than given by indirect low energy experiments.

Some issues should be addressed here:

- The purpose of this study is to demonstrate the potential of the LHeC experiments in probing RPV single squark resonance with even the most conservative estimations.

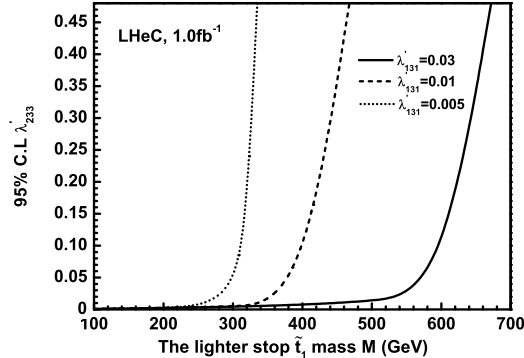


**Figure 7:** The upper bounds on  $\lambda'_{233}$  at given  $\lambda'_{131}$  as functions of stop masses at 70GeV  $e^-p$  collider.

Thus, the event selection strategy developed above is practicable and moderate, which is far from strict enough to optimize the signal significance. The constraints on R-violating  $\hat{L}\hat{Q}\hat{D}$  couplings derived are conservative and easy to achieve in experiment. For example, more severe muon b-jet mass window cut or binned likelihood method on  $M_{\mu b}$  can be employed while searching signal in high mass region, which would significantly improve sensitivity for  $M > 500\text{GeV}$  easily.

- The large signal cross section of positron configuration  $e^+p$  over electron beam  $e^-p$  in direct searching stop  $\tilde{t}_1$  quark resonance, is simply due to the large density of valance d-quark in proton. On the other hand, electron beams will take advantage over much larger luminosity; moreover, the single sbottom quark  $\tilde{b}$  resonance production and decay at the LHeC, i.e.  $e^- + p \rightarrow \tilde{b} \rightarrow \mu^- + u_k$  analogically could be dominant. Therefore, the electron beam configuration can provide excellent opportunity to probe  $\lambda'_{113}$  and  $\lambda'_{2k3}$  interactions.

#### 4. Summary

In this paper, the possibility of probing lepton flavor changing RPV  $\hat{L}\hat{Q}\hat{D}$  interactions via  $e + p \rightarrow \tilde{t} \rightarrow \mu + b$  process at the LHeC collider is investigated. Under the single dominance hypothesis, the resonance of stop quark can be produced and dominantly decay into muon and b-quark final states. An event selection strategy is developed to optimize the sensitivity of signal over SM background. Taking advantage of the enhancement of the direct resonance production of squark and the distinctive kinematics distributions between the signal and SM predictions, we come to conclusions that if there is no apparent excess of SM predictions on  $\mu + b$  final states, the sensitivity of RPV interactions can be measured at an unprecedented level compared to all the knowledge derived from indirect measurements.

**Acknowledgments:** This work was supported in part by the National Natural Science Foundation of China (No.11075150, No.11025528, No.11005101) and the Specialized



Research Fund for the Doctoral Program of Higher Education (No.20093402110030).

## References

- [1] Y. Fukuda *et al.* (Super-Kamiokande Collaboration), “Constraints on Neutrino Oscillations Using 1258 Days of Super-Kamiokande Solar Neutrino Data”, *Phys. Rev. Lett.* **86**, 5656 (2001).
- [2] Q. R. Ahmad *et al.* (SNO Collaboration), “Measurement of the Rate of  $\nu_e + d \rightarrow p + p + e^-$  Interactions Produced by  $^8B$  Solar Neutrinos at the Sudbury Neutrino Observatory”, *Phys. Rev. Lett.* **87**, 071301 (2001).
- [3] M. Apollonio *et al.* (CHOOZ Collaboration), “Limits on neutrino oscillations from the CHOOZ experiment”, *Phys. Lett. B* **466**, 415 (1999).
- [4] R. Barbier, C. Bérat, M. Besançon, M. Chemtob, A. Deandrea, E. Dudas, P. Fayet, S. Lavignac, G. Moreau, E. Perez, and Y. Sirois, “R-Parity-violating supersymmetry”, *Phys. Rept.* **420**, 1 (2005).
- [5] Y. B. Sun, L. Han, W. G. Ma, F. Tabbakh, R. Y. Zhang, and Y. J. Zhou, “Probing lepton flavor violation signal induced by R-violating minimal supersymmetric standard model at a linear collider”, *JHEP* **0409**, 043 (2004).
- [6] Y. B. Sun, Y. Jiang, J. R. Huang, L. Han, R. Y. Zhang, and W. G. Ma, “Probing R-parity Violating Interactions via  $p\bar{p} \rightarrow e\mu + X$  Channel on Tevatron”, *Commun. Theor. Phys.* **44**, 107 (2005).
- [7] S. M. Wang, L. Han, W. G. Ma, R. Y. Zhang, and Y. Jiang, “QCD corrections to the R-parity violating processes  $p\bar{p}/pp \rightarrow e\mu + X$  at hadron colliders”, *Phys. Rev. D* **74**, 057902 (2006).
- [8] S. M. Wang, L. Han, W. G. Ma, R. Y. Zhang, and Y. Jiang, “Revisiting the QCD Corrections to the R-Parity Violating Processes  $p\bar{p}/pp \rightarrow e\mu + X$ ”, *Chin. Phys. Lett.* **25**, 58 (2008).
- [9] A. Abulencia *et al.* (CDF Collaboration), “Search for High-Mass Resonances Decaying to  $e\mu$  in  $p\bar{p}$  Collisions at  $\sqrt{s} = 1.96$  TeV”, *Phys. Rev. Lett.* **96**, 211802 (2006).
- [10] V. Abazov *et al.* (DØ Collaboration), “Search for Scalar Neutrino Superpartners in  $e + \mu$  Final States in  $p\bar{p}$  Collisions at  $\sqrt{s} = 1.96$  TeV”, *Phys. Rev. Lett.* **100**, 241803 (2008).
- [11] J. B. Dainton, M. Klein, P. Newman, E. Perez, and F. Willeke, “Deep Inelastic Electron-Nucleon Scattering at the LHC”, *JINST* **1**, P10001 (2006).
- [12] E. Boos, V. Bunichev, M. Dubinin, L. Dudko, V. Edneral, V. Ilyin, A. Kryukov, V. Savrin, A. Semenov, and A. Sherstnev, “CompHEP 4.4-automatic computations from Lagrangians to events”, *Nucl. Instrum. Meth. A* **534** 250 (2004).
- [13] J. Pumplin, D. R. Stump, J. Huston, H. L. Lai, P. Nadolsky, and W. K. Tung, “New Generation of Parton Distributions with Uncertainties from Global QCD Analysis”, *JHEP* **0207**, 012 (2002).
- [14] D. Stump, J. Huston, J. Pumplin, W. K. Tung, H. L. Lai, S. Kuhlmann, and J. F. Owens, “Inclusive jet production, parton distributions, and the search for new physics”, *JHEP* **0310**, 046 (2003).